MSB(OH) as the predominant species, and the metal chelates present under these conditions are considered good candidates as active intermediates in oxidative deamination and are thus easy to identify. The α-deprotonated intermediate of the metal-Schiff base chelates formed from phenylglycine and its derivatives are expected to be stabilized by conjugation of the imine group with the phenyl ring on the α-carbon, and this property is one of the reason for selecting phenylglycine Schiff bases for oxidative deamination studies.

Acknowledgment. This research was supported by Grant AM-11694 from the National Institute of Arthritis, Diabetes, Digestive, and Kidney Diseases, U.S. Public Health Service, and by Grant A-259 from the Robert A. Welch Foundation. V.M.S. thanks Dr. R. J. Motekaitis for computational assistance.

Registry No. 3, 69-91-0; 4, 124755-49-3; 5, 2540-53-6; PLP, 54-47-7; DPL, 1849-49-6; PLP-PG, 124755-50-6; PLP-MPG, 124755-51-7; PLP-SPG, 124755-52-8; DPL-PG, 124755-53-9; DPL-MPG, 124755-54-0; DPL-SPG, 124755-55-1.

Contribution from the Department of Chemistry, University of Houston, Houston, Texas 77204-5641

Electrochemical and Spectroelectrochemical Characterization of Intermolecular Nitrosyl Transfer between Iron and Cobalt Porphyrins

X. H. Mu and K. M. Kadish*

Received March 10, 1989

The transfer of a nitrosyl ligand between neutral and oxidized iron and cobalt metalloporphyrins in dichloromethane solutions was investigated by electrochemistry and FTIR or ESR spectroelectrochemistry. The transfer of NO from (P)Co(NO) to (P)Fe, from $[(P)Co(NO)]^+$ to $(P)FeClO_4$, and from $[(P)Fe(NO)]^+$ to (P)Co was demonstrated for complexes where P = the dianion of tetraphenylporphyrin (TPP), *meso*-tetrakis(2,4,6-trimethylphenyl)porphyrin (TMP), or octaethylporphyrin (OEP). The driving force in these reactions is related to both the nature and oxidation state of the central metal in (P)M(NO) or $[(P)M(NO)]^+$, where M = Fe or Co, and follows the order (P)Fe(NO) > (P)Co(NO) > $[(P)Fe(NO)]^+$ > $[(P)Co(NO)]^+$.

Introduction

Numerous spectroscopic,[1-11] structural,[12-18] and electrochemical[19-32] studies of neutral and oxidized iron and cobalt nitrosyl porphyrins have been reported in the literature. These compounds are represented by (P)M(NO) and $[(P)M(NO)]^+$, where M = Co(II), Fe(II), or Fe(III) and P is the dianion of a given porphyrin ring.

Intermolecular NO transfer between two coordinatively unsaturated transition-metal complexes is of interest in both inorganic and bioinorganic chemistry[33-35] and has been shown to occur through formation of a transient μ-bridged nitrosyl complex. The transfer of NO from a non-porphyrin complex to hemoglobin was reported by Doyle,[35] but an NO transfer between two metalloporphyrins has never been demonstrated.

In this paper, we present the first examples for NO-transfer reactions between Fe and Co metalloporphyrins. The investigated reactions are given by eqs 1-3, where P is the dianion of tetraphenylporphyrin (TPP), *meso*-tetrakis(2,4,6-trimethylphenyl)porphyrin (TMP), or octaethylporphyrin (OEP). Each of the above reactions was monitored in CH_2Cl_2 by thin-layer and conventional electrochemistry as well as by FTIR or ESR spectroelectrochemistry.

$$(P)Fe + (P)Co(NO) \rightarrow (P)Fe(NO) + (P)Co \quad (1)$$

$$(P)Co + [(P)Fe(NO)]^+ \rightarrow (P)Co(NO) + (P)FeClO_4 \quad (2)$$

$$(P)FeClO_4 + [(P)Co(NO)]^+ \rightarrow [(P)Fe(NO)]^+ + (P)CoClO_4 \quad (3)$$

To date, there are only two reports in the literature involving the transfer of a nitrogen atom between two metalloporphyrins.

(1) Yoshimura, T. *Inorg. Chem.* **1986**, *25*, 688.
(2) Perutz, M. F.; Kilmartin, J. V.; Nagai, K.; Szabo, A.; Simon, S. R. *Biochemistry* **1976**, *15*, 378.
(3) Wayland, B. B.; Olson, L. W. *J. Am. Chem. Soc.* **1974**, *96*, 6037.
(4) Wayland, B. B.; Minkiewicz, J. V.; Abd-Elmageed, M. E. *J. Am. Chem. Soc.* **1974**, *96*, 2795.
(5) Wayland, B. B.; Olson, L. W. *J. Chem. Soc., Chem. Commun.* **1973**, 897.
(6) Wayland, B. B.; Minkiewitz, J. V. *J. Chem. Soc., Chem. Commun.* **1976**, 1015.
(7) Yoshimura, T.; Ozaki, T. *Arch. Biochem. Biophys.* **1984**, *229*, 126-235.
(8) Yoshimura, T. *Bull. Chem. Soc. Jpn.* **1983**, *56*, 2527.
(9) Yoshimura, T. *Inorg. Chim. Acta* **1984**, *83*, 17-21.
(10) Brault, D.; Rougee, M. *Biochemistry* **1974**, *13*, 4591.
(11) Gibson, Q. H. In *The Porphyrins*; Dolphin, D., Ed.; Academic Press: New York, 1978; Vol. V, Chapter 5, p 153.
(12) Scheidt, W. R.; Frisse, M. E. *J. Am. Chem. Soc.* **1975**, *97*, 17.
(13) Scheidt, W. R.; Hoard, J. L. *J. Am. Chem. Soc.* **1973**, *95*, 8281.
(14) Piciulo, P. L.; Scheidt, W. R. *J. Am. Chem. Soc.* **1976**, *98*, 1913.
(15) Scheidt, W. R.; Brineger, A. C.; Ferro, E. B.; Kirner, J. F. *J. Am. Chem. Soc.* **1977**, *99*, 7315.
(16) Scheidt, W. R.; Lee, Y. J.; Hatano, K. *J. Am. Chem. Soc.* **1984**, *106*, 3191.
(17) Piciulo, P. L.; Rupprecht, G.; Scheidt, W. R. *J. Am. Chem. Soc.* **1974**, *96*, 5293.
(18) Scheidt, W. R.; Lee, Y. J. *Struct. Bonding (Berlin)* **1987**, *64*, 1-70.
(19) Olson, L. W.; Schaeper, D.; Lançon, D.; Kadish, K. M. *J. Am. Chem. Soc.* **1982**, *104*, 2042.
(20) Lançon, D.; Kadish, K. M. *J. Am. Chem. Soc.* **1983**, *105*, 5610.
(21) Kelly, S.; Lançon, D.; Kadish, K. M. *Inorg. Chem.* **1984**, *23*, 1451.
(22) Mu, X. H.; Kadish, K. M. *Inorg. Chem.* **1988**, *27*, 4720.
(23) Kadish, K. M.; Mu, X. H.; Lin, X. Q. *Inorg. Chem.* **1988**, *27*, 1489.
(24) Kadish, K. M.; Mu, X. H.; Lin, X. Q. *Electroanalysis* **1988**, *1*, 35.
(25) Fujita, E.; Fajer, J. *J. Am. Chem. Soc.* **1983**, *105*, 6743.
(26) Fujita, E.; Chang, C. K.; Fajer, J. *J. Am. Chem. Soc.* **1985**, *107*, 7665.
(27) Choi, I. K.; Ryan, M. D. *Inorg. Chim. Acta* **1988**, *153*, 25.
(28) Feng, D. W.; Ryan, M. D. *Inorg. Chem.* **1987**, *26*, 2480.
(29) Fernandes, J. B.; Feng, D. W.; Chang, A.; Keyser, A.; Ryan, M. D. *Inorg. Chem.* **1986**, *25*, 2606.
(30) Guilard, R.; Lagrange, G.; Tabard, A.; Lançon, D.; Kadish, K. M. *Inorg. Chem.* **1985**, *24*, 3649.
(31) Barley, M. H.; Takeuchi, K. J.; Murphy, W. R., Jr.; Meyer, T. J. *J. Chem. Soc., Chem. Commun.* **1985**, 507.
(32) Barley, M. H.; Takeuchi, K. J.; Meyer, T. J. *J. Am. Chem. Soc.* **1986**, *108*, 5876.
(33) Ungermann, C. B.; Caulton, K. G. *J. Am. Chem. Soc.* **1976**, *98*, 3862.
(34) Doyle, M. P.; Van Doornik, F. J.; Funckes, C. L. *Inorg. Chim. Acta* **1980**, *46*, L111.
(35) Doyle, M. P.; Pickering, R. A.; Dykstra, R. L.; Cook, B. R. *J. Am. Chem. Soc.* **1982**, *104*, 3392.

0020-1669/90/1329-1031$02.50/0

These reactions involve complexes with different porphyrin rings and different central metals[36] or between metalloporphyrins with the same central metal and different porphyrin rings.[37] An example of these reactions is shown in eq 4, where TTP is the dianion of *meso*-tetra-*p*-tolylporphyrin and M = Mn or Cr.[37]

$$(TTP)M^{V}(N) + (OEP)M^{II} \rightleftarrows (OEP)M^{V}(N) + (TTP)M^{II} \quad (4)$$

The driving force in reaction 4 is the difference in basicity between the OEP and TTP porphyrin rings, and this is also directly related to redox potentials for oxidation of $(OEP)M^{II}$ or reduction of $(TTP)M^{V}(N)$ under the same experimental conditions. The driving force in reactions 1–3 is related in part to differences in porphyrin ring basicity but is more strongly influenced by the presence of two different central metals (Co and Fe) and the different oxidation states of the central metal ions.

Experimental Section

Materials. (TPP)Fe(NO), (TMP)Fe(NO), (OEP)Fe(NO),[19,22] and (TPP)Co(NO)[13] were synthesized and characterized by published procedures from $(TPP)FeClO_4$, $(TMP)FeClO_4$, $(OEP)FeClO_4$, and (TPP)Co. All of the nitrosyl complexes are air stable in the solid state. (P)Fe was in situ generated by controlled-potential electroreduction of $(P)FeClO_4$ in a thin-layer cell, while $[(P)Fe(NO)]^+$ and $[(P)Co(NO)]^+$ were produced by electrooxidation of neutral (P)Fe(NO) and (P)Co(NO) under the same experimental conditions. Methylene chloride (CH_2Cl_2) (analytical grade, Fisher Scientific Co.) was freshly distilled from P_2O_5 before use. Tetrabutylammonium perchlorate (TBAP, Fluka Chemical Co.) was used as supporting electrolyte and was twice recrystallized from ethanol and dried in vacuo prior to use.

Instrumentation and Procedure. Cyclic voltammograms were obtained with an IBM Model 225A voltammetric analyzer and an Omnigraphic 2000 X-Y recorder. A three-electrode thin-layer electrochemical cell was utilized and consisted of a platinum-gauze working electrode, a platinum-gauze auxiliary electrode, and a homemade saturated calomel electrode (SCE) as the reference electrode.[38] A positive pressure of high-purity nitrogen was kept above the solution during the experiment. Uncompensated *iR* drop in the solution was minimized by use of a positive feedback device built into the IBM Model 225A.

FTIR spectra were measured in CH_2Cl_2, 0.1 M TBAP by using an IBM IR 32 FTIR spectrometer and a light-transparent spectroelectrochemical three-electrode IR cell. The application[22,23] and construction[24] of this cell have been described in the literature. A solution containing CH_2Cl_2 and 0.1 M TBAP was used to provide the background spectrum. The FTIR spectrum of a solution containing 0.5–2.0 mM of the iron or cobalt porphyrins was taken as the reference spectrum in difference FTIR spectroelectrochemical measurements. Positive peaks in the FTIR difference spectra (sample spectrum minus reference spectrum) are due to an electrogenerated species, while negative peaks correspond to a disappearance of the reactant upon electrooxidation or electroreduction in the thin-layer cell.

ESR experiments were carried out with a homebuilt three-electrode cell, and spectral monitoring was carried out with an IBM ER 100D spectrometer.

Results and Discussion

Nitrosyl Transfer from (TPP)Co(NO) to (P)Fe. Parts a and b of Figure 1 show thin-layer cyclic voltammograms of 5.0×10^{-4} M $(OEP)FeClO_4$ and 5.0×10^{-4} M (OEP)Fe(NO) in CH_2Cl_2, 0.1 M TBAP. $(OEP)FeClO_4$ undergoes a reversible one-electron reduction at $E_{1/2} = 0.05$ V, while (OEP)Fe(NO) is reversibly oxidized at $E_{1/2} = 0.61$ V under the same experimental conditions. These redox potentials and those of related cobalt and iron porphyrins in CH_2Cl_2 are listed in Table I.

The voltammogram for a mixture of 5.0×10^{-4} M $(OEP)FeClO_4$ and 5.0×10^{-4} M (TPP)Co(NO) in CH_2Cl_2, 0.1 M TBAP is shown in Figure 1c. The reduction of $(OEP)FeClO_4$ is irreversible in the presence of (TPP)Co(NO) and occurs at $E_p = 0.09$ V to generate (OEP)Fe. The shape of the reduction peak is well defined in Figure 1c but the reduction potential is positively shifted from that of the pure compound (Figure 1a), consistent with the occurrence of a rapid chemical reaction following the electron-transfer step. There is no return oxidation peak coupled to the reduction peak of $(OEP)FeClO_4$, and an analysis of the current–voltage curve is consistent with an electrochemical EC type reduction mechanism.[39]

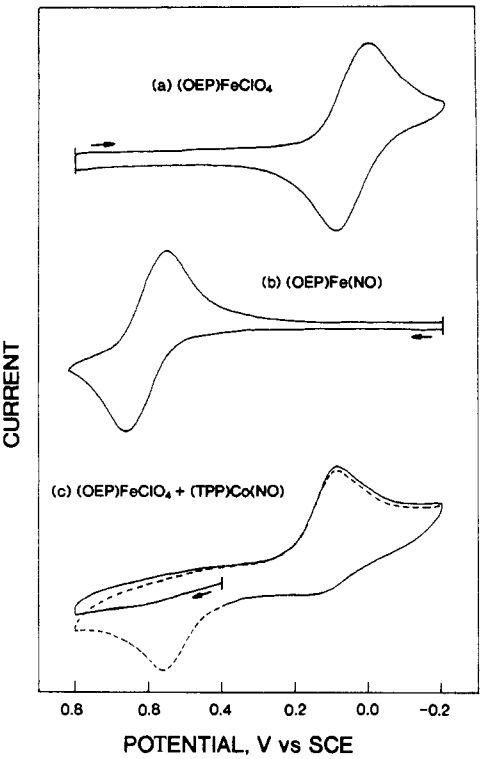

Figure 1. Thin-layer cyclic voltammograms of (a) 5.0×10^{-4} M $(OEP)FeClO_4$, (b) 5.0×10^{-4} M (OEP)Fe(NO), and (c) a mixture containing 5.0×10^{-4} M (TPP)Co(NO) and 5.0×10^{-4} M $(OEP)FeClO_4$ in CH_2Cl_2, 0.1 M TBAP. Scan rate = 10 mV/s.

Table I. Half-Wave Potentials for the Oxidation and Reduction of Iron[a] and Cobalt[b] Porphyrins in CH_2Cl_2, 0.1 M TBAP

compd	1st oxidn	1st redn	ref
(TPP)Co(NO)	1.01	−1.18	21
(TPP)Co	0.75	−0.85	46
(OEP)Fe(NO)	0.60	−1.08	19, 22
$(OEP)FeClO_4$	1.02	0.10	47
(TPP)Fe(NO)	0.74	−0.93	19, 22
$(TPP)FeClO_4$	1.11	0.24	19
(TMP)Fe(NO)	0.67	−1.15	22
$(TMP)FeClO_4$	1.09	0.16	48

[a] The first oxidation and first reduction of each $(P)FeClO_4$ complex occurs at the porphyrin π ring system and central metal ion, respectively. The first oxidation of (P)Fe(NO) generates an Fe(III) species, but the first reduction of this complex may occur at either the central Fe or at the axial NO ligand. [b] The first reduction of (TPP)Co occurs at the central metal ion, while the first oxidation and first reduction of (TPP)Co(NO) occurs at the porphyrin π ring system. The first oxidation of (TPP)Co can occur either at the central metal ion or at the porphyrin π ring system, depending upon the solvent properties.[49–51]

An oxidation peak is not observed in Figure 1c when the potential is first scanned from 0.40 to 0.80 V. However, when a second positive scan is initiated after the formation of (OEP)Fe in the thin-layer chamber, an oxidation at $E_p = 0.56$ V is observed (see dashed line in Figure 1c). This electrode reaction is assigned to the oxidation of (OEP)Fe(NO), which is homogeneously generated in solution according to eqs 5 and 6.

$$(OEP)FeClO_4 + e^- \rightleftarrows (OEP)Fe + ClO_4^- \quad (5)$$

$$(OEP)Fe + (TPP)Co(NO) \rightarrow (OEP)Fe(NO) + (TPP)Co \quad (6)$$

(36) Bottomley, L. A.; Neely, F. L. *J. Am. Chem. Soc.* **1989**, *111*, 5955.
(37) Woo, L. K.; Goll, J. G. *J. Am. Chem. Soc.* **1989**, *111*, 3755.
(38) Lin, X. Q.; Kadish, K. M. *Anal. Chem.* **1985**, *57*, 1498.
(39) Nicholson, R. S.; Shain, I. *Anal. Chem.* **1964**, *36*, 706.

Table II. NO Vibration Frequencies[a] (cm^{-1}) of (P)M(NO) and $[(P)M(NO)]^+$ in CH_2Cl_2, 0.1 M TBAP[b]

complex	ν_{NO}(pure compds)[c]	ν_{NO}(mixtures) (TPP)Co(NO) + (OEP)$FeClO_4$	(TPP)Co(NO) + (TPP)$FeClO_4$	(TPP)Co(NO) + (TMP)$FeClO_4$	(TPP)Co + (OEP)Fe(NO)
(TPP)Co(NO)	1684	1684	1684	1684	1689 (0.7)
(OEP)Fe(NO)	1667	1663 (−0.2)			1667
(TMP)Fe(NO)	1672			1674 (−0.2)	
(TPP)Fe(NO)	1678		1676 (−0.2)		
$[(TPP)Co(NO)]^+$	1726	1726 (1.1)	1726 (1.1)	1726 (1.1)	
$[(OEP)Fe(NO)]^+$	1854	1852 (1.1)			1854 (0.7)
$[(TMP)Fe(NO)]^+$	1838			1838 (1.1)	
$[(TPP)Fe(NO)]^+$	1848		1850 (1.1)		

[a] Data good as ±2 cm^{-1}. [b] Values in parentheses are the controlled potentials that were applied to the given solution before taking the IR measurement. [c] Taken from refs 22 and 23.

Scheme I

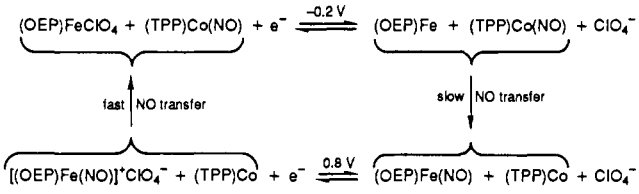

As seen in Figure 1b, the thin-layer oxidation of (OEP)Fe(NO) occurs at $E_{1/2}$ = 0.61 V, and this is consistent with data in the literature for reactions of the same compound at a conventional electrode.[20] In contrast, the oxidation of chemically generated (OEP)Fe(NO) in a thin-layer cell is irreversible and occurs at E_p = 0.56 V (see Figure 1c). The shape of the peak is well defined, and the lack of a return rereduction peak and the negative potential shift for the oxidation of (OEP)Fe(NO) are both consistent with an EC type oxidation mechanism. The difference in behavior between the oxidative voltammogram in Figure 1b and that in Figure 1c is due to the fact that electrogenerated $[(OEP)Fe(NO)]^+$ undergoes an NO transfer with (TPP)Co to give (TPP)Co(NO) as a final NO product in solution. This reaction occurs as shown in eq 2.

The overall sequence of electrochemical and chemical steps in Figure 1c involves an ECEC type mechanism and results in a re-formation of the original solution mixture after a controlled-potential reduction at −0.2 V followed by a controlled-potential oxidation at 0.8 V. This box mechanism is illustrated by Scheme I.

The above two NO-transfer reactions occur directly between the two metalloporphyrins without a preceding NO dissociation. The intermediate of these reactions most likely involves a μ-bridged Co–NO–Fe species, as has been reported in the literature for other NO transfer reactions.[35]

The data by conventional cyclic voltammetry indicate that the NO transfer between $[(OEP)Fe(NO)]^+$ and (TPP)Co (reaction 2) is much faster than the NO transfer between (TPP)Co(NO) and (OEP)Fe (reaction 1). The reduction of (OEP)$FeClO_4$ at a potential scan rate of 0.1 V/s shows a ratio of anodic to cathodic peak current of ~0.5 in CH_2Cl_2 containing equimolar (OEP)$FeClO_4$ and (TPP)Co(NO). This indicates that the transfer of NO from (TPP)Co(NO) to electrogenerated (OEP)Fe is ~50% complete in ~5 s for a solution containing 5.0 × 10^{-4} M of each metalloporphyrin.

In contrast, there is no rereduction peak for electrooxidized $[(OEP)Fe(NO)]^+$ at any scan rate up to 10 V/s in CH_2Cl_2 solutions containing 5.0 × 10^{-4} M (TPP)Co. This is consistant with a transfer of NO from $[(OEP)Fe(NO)]^+$ to (TPP)Co in less than 0.04 s. Thus, the transfer of an NO ligand from $[(OEP)Fe(NO)]^+$ to (TPP)Co in CH_2Cl_2, 0.1 M TBAP is more than 100 times faster than the transfer of an NO ligand from (TPP)Co(NO) to (OEP)Fe under the same experimental conditions and is consistent with the increased lability of the singly oxidized species.

The two nitrosyl-transfer reactions shown in the above scheme were also monitored by in situ FTIR spectroelectrochemistry under the same experimental conditions. (TPP)Co(NO) shows a strong

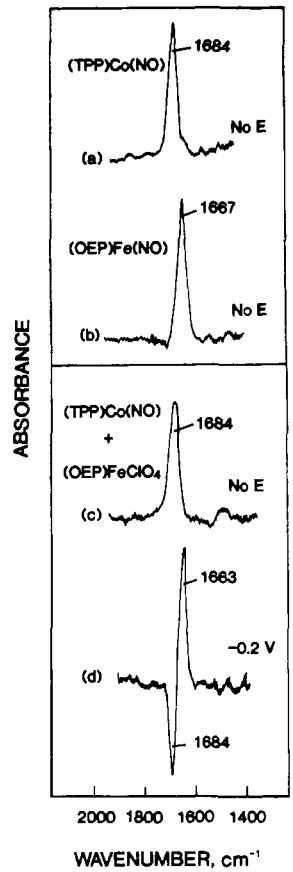

Figure 2. FTIR spectra of (a) (TPP)Co(NO), (b) (OEP)Fe(NO), and (c) a mixture containing 5.0 × 10^{-4} M (TPP)Co(NO) and 5.0 × 10^{-4} M (OEP)$FeClO_4$ in CH_2Cl_2, 0.1 M TBAP and (d) FTIR difference spectrum of a mixture containing 5.0 × 10^{-4} M (TPP)Co(NO) and 5.0 × 10^{-4} M (OEP)$FeClO_4$ after controlled-potential reduction at −0.2 V.

NO vibration band at 1684 cm^{-1} in CH_2Cl_2, 0.1 M TBAP (see Figure 2a), while the NO vibration of (OEP)Fe(NO) in CH_2Cl_2 is located at 1667 cm^{-1}. FTIR spectra for pure solutions of these compounds are shown in Figure 2a,b.

Parts c and d of Figure 2 show FTIR spectra for a mixture of (TPP)Co(NO) and (OEP)$FeClO_4$ in CH_2Cl_2, 0.1 M TBAP before and after controlled-potential reduction. The 1684-cm^{-1} NO vibration of (TPP)Co(NO) disappears after controlled-potential reduction at −0.2 V (see negative peak in Figure 2d) and is accompanied by a strong positive absorption peak of the product, which appears at 1663 cm^{-1}. This later peak is assigned as due to chemically generated (OEP)Fe(NO) and can be compared to the 1667-cm^{-1} NO vibration of pure (OEP)Fe(NO) in the absence of a cobalt porphyrin (see Figure 2b).

Similar NO-exchange reactions were obtained between (TPP)Fe and (TPP)Co(NO) and between (TMP)Fe and (TPP)Fe(NO) in CH_2Cl_2. The IR data to support these assignments are listed in Table II.

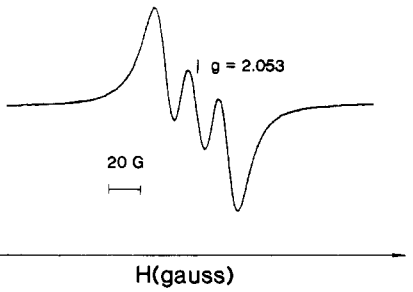

Figure 3. Room-temperature ESR spectrum of a mixture containing 5.0 × 10^{-4} M (TPP)Co(NO) and 5.0 × 10^{-4} M (OEP)$FeClO_4$ in CH_2Cl_2, 0.1 M TBAP after controlled-potential reduction at −0.2 V.

ESR spectroelectrochemistry was also used to monitor the series of reactions given by eqs 5 and 6. The initial mixture of (OEP)$FeClO_4$ and (TPP)Co(NO) is ESR silent at room temperature,[40] but after electroreduction at −0.2 V, a well-defined ESR signal is observed. This spectrum (shown in Figure 3) has g = 2.053 and an $^{14}N(NO)$ hyperfine splitting constant of 16.9 G. The ESR spectrum is comparable with the one reported for (TPP)Fe(NO) (g = 2.054, $^{14}N(NO)$ = 17.4 G)[3,5] as well as with other iron nitrosyl porphyrin complexes.[1,41] Thus, the ESR data confirm the homogeneous generation of (OEP)Fe(NO) after controlled-potential electroreduction of a CH_2Cl_2 solution containing (OEP)$FeClO_4$ and (TPP)Co(NO).

Clearly, the driving force for the nitrosyl-transfer reactions in eqs 1–3 is related to both the nature and oxidation state of the central metal ions in the (P)M(NO) or $[(P)M(NO)]^+$ complexes. A comparison of data in this present study with available structural data for (TPP)Fe(NO) and (TPP)Co(NO) also suggests that the NO-transfer reactions should be related, at least to some extent, to the bond strengths of Fe–NO and Co–NO.

Theoretically, the extent of back electron donation from a transition metal to a bound NO group leads to a stronger M–NO bond and a weaker N–O bond. This is reflected by a shorter M–NO bond, a longer N–O bond, and a lower NO vibration frequency.[42] Wayland[3,4] has reported that linear diatomic molecule adducts of cobalt and iron metalloporphyrins have maximum π–π interaction between the central metal and the diatomic molecule, thus making the bond between them stronger.

The NO vibration frequencies of (P)Fe(NO) and (P)Co(NO) also depend upon the extent of π–π interaction.[3,42] (TPP)Fe(NO) has an Fe–N–O angle of 149.2°, and this can be compared to a Co–N–O bond angle of 128.5° in (TPP)Co(NO). Thus, (TPP)Fe(NO) should have a larger π–π interaction between the iron and nitric oxide than does (TPP)Co(NO). This is indeed the case, as indicated by the Fe–NO bond length (1.717 Å),[12] which is shorter than the Co–NO bond length (1.833 Å).[13] The FeN–O bond length of 1.122 Å is longer than CoN–O bond length (1.01 Å), and the NO vibration frequency of (TPP)Fe(NO) in either the solid state (1670 cm^{-1})[12] or in CH_2Cl_2 solutions (1678 cm^{-1})[22] is at lower frequency than the NO vibration frequency of (TPP)Co(NO) in the solid state (1689 cm^{-1})[13] or in CH_2Cl_2 solutions (1684 cm^{-1}).[24] Thus, all of the data agree with theoretical predictions[3,42] and indicate that an NO transfer between (P)Co(NO) and (P)Fe should be possible.

The above discussion on cobalt and iron nitrosyl porphyrin complexes does not appear to extend to the nitrosyl complexes of Mn. Structural data for (TTP)Mn(NO)[43] show that the complex has a shorter Mn–NO bond and a more linear Mn–N–O angle than does the corresponding (TPP)Fe(NO) species. Thus, one might suggest that (P)Mn should accept an NO ligand from either (P)Fe(NO) or (P)Co(NO). These reactions were attempted in the present study. However, under our experimental conditions (CH_2Cl_2, 0.1 M TBAP) an NO-transfer reaction did not occur between (OEP)Fe(NO) and (TPP)Mn or between (TPP)Co(NO) and (TPP)Mn on the cyclic voltammetric time scale. These negative results indicate that neither the bond strength of M–NO nor the linearity of M–N–O seem to be key factors that determine the observed NO-transfer reactions. The more dominant factors must be related to the nature and/or oxidation state of the central metal ions. Other factors such as the electron configuration[21] of the complex may also play a role. In fact, (P)Mn(NO)[43] and $[(P)Mn(NO)]^+$[21] are far more reactive than their corresponding Fe and Co derivatives.

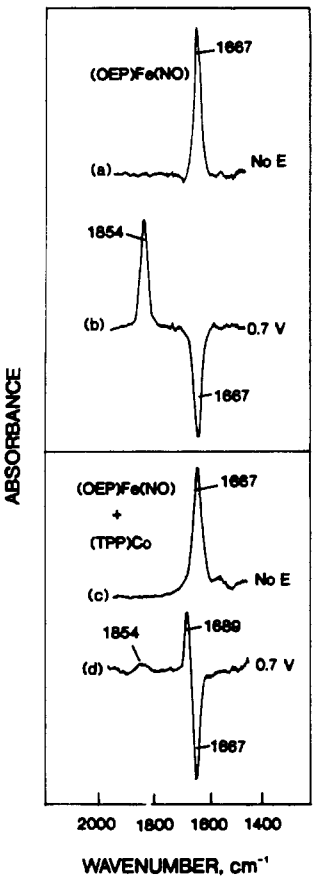

Figure 4. (a) FTIR spectrum of (OEP)Fe(NO) in CH_2Cl_2, 0.1 M TBAP, (b) FTIR difference spectrum of (OEP)Fe(NO) after electrooxidation at 0.7 V, (c) FTIR spectrum of a mixture containing 5.0 × 10^{-4} M (OEP)Fe(NO) and 5.0 × 10^{-4} M (TPP)Co in CH_2Cl_2, 0.1 M TBAP, and (d) FTIR difference spectrum of a mixture containing 5.0 × 10^{-4} M (OEP)Fe(NO) and 5.0 × 10^{-4} M (TPP)Co in CH_2Cl_2, 0.1 M TBAP after controlled-potential oxidation at 0.7 V.

Nitrosyl Transfer from $[(OEP)Fe(NO)]^+$ to (TPP)Co. The NO-transfer reaction between $[(OEP)Fe(NO)]^+$ and (TPP)Co has already been discussed with respect to its influence on thin-layer cyclic voltammograms for the oxidation of homogeneously generated (OEP)Fe(NO) (see Figure 1c). This exchange reaction was also monitored by using thin-layer FTIR spectroelectrochemistry.

Parts a and b of Figure 4 show FTIR spectra of (OEP)Fe(NO) before and after electrooxidation at 0.7 V in CH_2Cl_2, 0.1 M TBAP. The initial (OEP)Fe(NO) complex has an NO vibration at 1667 cm^{-1}, while the NO vibration of $[(OEP)Fe(NO)]^+$ is at 1854 cm^{-1}. FTIR spectra of these compounds are shown in Figure 4a,b. Parts c and d of Figure 4 show FTIR spectra for a mixture containing 5.0 × 10^{-4} M (OEP)Fe(NO) and 5.0 × 10^{-4} M (TPP)Co before and after controlled-potential oxidation at 0.7 V. Only a single peak is observed at 1667 cm^{-1} prior to electrooxidation (Figure 4c), and this can be assigned as the NO vibration of (OEP)Fe(NO). An application of 0.7 V to this solution leads to the generation of $[(OEP)Fe(NO)]^+$ (eq 7), but this Fe(III) complex

(40) The ESR spectrum of (OEP)$FeClO_4$ is not detectable at room temperature. See: Dolphin, D. H.; Sams, J. R.; Tsin, T. B. *Inorg. Chem.* **1977**, *16*, 711.
(41) Yoshimura, T. *Arch. Biochem. Biophys.* **1983**, *220*, 167.
(42) Cotton, F. A.; Wilkinson, G. *Advanced Inorganic Chemistry*, 5th ed.; John Wiley and Sons: New York, 1988; Chapter 2.
(43) Scheidt, W. R.; Hatano, K.; Rupprecht, G. A.; Piciulo, P. L. *Inorg. Chem.* **1979**, *18*, 292.

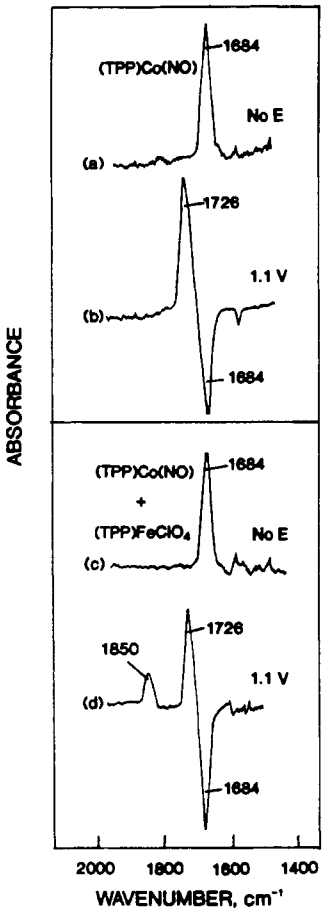

Figure 5. (a) FTIR spectrum of (TPP)Co(NO) in CH_2Cl_2, 0.1 M TBAP, (b) FTIR difference spectrum of (TPP)Co(NO) in CH_2Cl_2, 0.1 M TBAP after controlled-potential oxidation at 1.1 V, (c) FTIR spectrum of 5.0×10^{-4} M (TPP)Co(NO) and 5.0×10^{-4} M (TPP)$FeClO_4$ in CH_2Cl_2, 0.1 M TBAP, and (d) FTIR difference spectra of 5.0×10^{-4} M (TPP)Co(NO) and 5.0×10^{-4} M (TPP)$FeClO_4$ in CH_2Cl_2, 0.1 M TBAP after controlled-potential oxidation at 1.1 V.

rapidly transfers the NO to (TPP)Co and gives (TPP)Co(NO) as a final product, as shown in eq 8.

$$(OEP)Fe(NO) \rightleftharpoons [(OEP)Fe(NO)]^+ + e^- \quad (7)$$

$$[(OEP)Fe(NO)]^+ + (TPP)Co \rightarrow (OEP)FeClO_4 + (TPP)Co(NO) \quad (8)$$

The above nitrosyl transfer leads to the difference FTIR spectrum shown in Figure 4d. The homogeneously generated (TPP)Co(NO) has an NO vibration at 1689 cm^{-1}, which compares to a value of 1684 cm^{-1} in the mixture (see Figure 2a).

Nitrosyl Transfer from $[(TPP)Co(NO)]^+$ to (P)$FeClO_4$. A structural characterization of $[(P)Co(NO)]^+$ has not been published, but solution data indicate that the Fe–NO bond of $[(P)Fe(NO)]^+$ is stronger than the Co–NO bond of $[(P)Co(NO)]^+$. For example, $[(TPP)Fe(NO)(Me_2SO)]^+$ is stable in CH_2Cl_2 containing 5.0×10^{-2} M Me_2SO[22,24] but $[(TPP)Co(NO)(Me_2SO)]^+$ is not stable under the same experimental conditions[24] and $[(TPP)Co(Me_2SO)_2]^+$ is formed after a rapid dissociation of the NO group. Likewise, $[(TPP)Fe(NO)]^+$ is quite stable in PhCN[20] but a displacement of NO by PhCN is rapidly observed after the electrochemical conversion of (TPP)Co(NO) to $[(TPP)Co(NO)]^+$ in PhCN.[44] All of these data indicate that one might expect to observe a nitrosyl transfer between $[(P)Co(NO)]^+$ and (P)$FeClO_4$ in CH_2Cl_2. This is indded the case, as discussed in the following paragraphs.

Parts a and b of Figure 5 show the FTIR spectrum of (TPP)Co(NO) before and after electrooxidation, while parts c and d of Figure 5 show the spectrum for a mixture of 5.0×10^{-4} M

(44) Kadish, K. M.; Mu, X. H. Unpublished results.

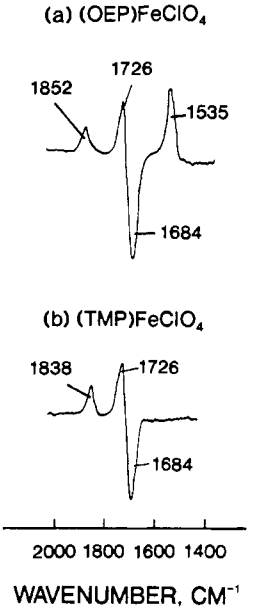

Figure 6. FTIR difference spectra after controlled-potential oxidation at 1.1 V of a mixture containing 5.0×10^{-4} M (TPP)Co(NO) and (a) 5.0×10^{-4} M (OEP)$FeClO_4$ or (b) 5.0×10^{-4} M (TMP)$FeClO_4$ in CH_2Cl_2, 0.1 M TBAP.

(TPP)Co(NO) and 5.0×10^{-4} M (TPP)$FeClO_4$ before and after controlled-potential oxidation at 1.1 V. The electrode reactions that occur at this potential are given by eqs 9 and 10.

$$(TPP)Co(NO) \xrightleftharpoons{E_{1/2} = 1.01\ V} [(TPP)Co(NO)]^+ + e^- \quad (9)$$

$$(TPP)FeClO_4 \xrightleftharpoons{E_{1/2} = 1.11\ V} [(TPP)FeClO_4]^+ + e^- \quad (10)$$

The difference FTIR spectrum in Figure 5d has a negative peak at 1684 cm^{-1} and two positive peaks at 1726 and 1850 cm^{-1}. The 1726-cm^{-1} peak is due to $[(TPP)Co(NO)]^+$, while the 1850-cm^{-1} peak is due to $[(TPP)Fe(NO)]^+$, which is generated as shown in eq 11.

$$(TPP)FeClO_4 + [(TPP)Co(NO)]^+ \rightarrow [(TPP)Fe(NO)]^+ + (TPP)CoClO_4 \quad (11)$$

The sum intensities of the positive 1726- and 1850-cm^{-1} peaks are about the same as the intensity of the negative 1684-cm^{-1} peak in Figure 5d and indicate that the solution contains a mixture of $[(TPP)Co(NO)]^+$ and $[(TPP)Fe(NO)]^+$. The obtaining of a mixture is due to the fact that a potential of about 1.1 V is needed to quantitatively convert (TPP)Co(NO) to $[(TPP)Co(NO)]^+$, but at this potential, the oxidation of (TPP)$FeClO_4$ to $[(TPP)FeClO_4]^+$ also occurs.

The $E_{1/2}$ for the conversion of (TPP)$FeClO_4$ to $[(TPP)FeClO_4]^+$ is 1.11 V, and therefore about 50% of (TPP)$FeClO_4$ is oxidized to $[(TPP)FeClO_4]^+$ at an applied potential of 1.1 V. The remaining 50% of (TPP)$FeClO_4$ reacts with electrogenerated $[(TPP)Co(NO)]^+$ to produce $[(TPP)Fe(NO)]^+$ in solution. Both $[(TPP)Co(NO)]^+$ and $[(TPP)Fe(NO)]^+$ are stable at this applied potential,[20-23] and both complexes are spectrally detected.

The nitrosyl-transfer reactions between $[(TPP)Co(NO)]^+$ and (P)$FeClO_4$ where P = OEP or TMP were also monitored. The difference IR spectra recorded after these NO transfers are shown in Figure 6a,b and are similar to the spectrum given in Figure 5d for the reaction of $[(TPP)Co(NO)]^+$ with (TPP)$FeClO_4$. In all three cases, there is a negative peak at 1684 cm^{-1} and a positive peak at 1726 cm^{-1}. These two peaks are independent of the iron porphyrin macrocycle (OEP or TMP) and are due to the neutral (TPP)Co(NO) (1684 cm^{-1}) and its electrooxidized product, $[(TPP)Co(NO)]^+$ (1726 cm^{-1}). The iron nitrosyl complex, $[(P)Fe(NO)]^+$, is also a product in this NO-transfer reaction, and the peak for this species varies as a function of the specific porphyrin ring. A positive NO peak appears at 1852 cm^{-1} for the (TPP)Co(NO)/(OEP)$FeClO_4$ system, while a peak is located at

1838 cm^{-1} for the (TPP)Co(NO)/(TMP)$FeClO_4$ system. The former peak is due to $[(OEP)Fe(NO)]^+$, while the latter is due to $[(TMP)Fe(NO)]^+$.

A positive peak at 1535 cm^{-1} (see Figure 6a) only occurs for the exchange reaction involving (OEP)$FeClO_4$ and $[(TPP)Co(NO)]^+$ and is assigned as the π-cation-radical marker band of $[(OEP)FeClO_4]^+$, which is generated at 1.1 V according to eq 12.[22,45]

$$(OEP)FeClO_4 \overset{E_{1/2} = 1.02\ V}{\rightleftharpoons} [(OEP)FeClO_4]^+ + e^- \quad (12)$$

Conclusion. A nitrosyl ligand transfer can be observed between Fe(II) and Co(II) porphyrins, between Co(II) and Fe(III) porphyrins, and between Fe(III) porphyrins and Co(II) porphyrin cation radicals. The driving force behind these different NO-transfer reactions is related both to the nature of the different central metals of (P)M(NO) and $[(P)M(NO)]^+$ and to the different oxidation states of the complex. The NO transfer is also related to differences in the porphyrin macrocycle although, in the present series of investigated compounds, this effect was not dominant. In summary, the following overall order of stability is observed for the investigated nitrosyl complexes:

$$(P)Fe(NO) > (P)Co(NO) > [(P)Fe(NO)]^+ > [(P)Co(NO)]^+$$

Finally, the data and observations reported in the present paper should prove helpful in understanding the reactions of these biologically important species and should also serve as a basis for comparing other published data on metalloporphyrins containing diatomic molecule adducts.

Acknowledgment. The support of the National Institutes of Health (Grant GM-15172) and the National Science Foundation (Grant CHE-8822881) is gratefully acknowledged.

Registry No. NO, 14452-93-8; (OEP)$FeClO_4$, 50540-30-2; (OEP)Fe(NO), 55917-58-3; (TPP)Co(NO), 42034-08-2; $[(OEP)Fe(NO)]^+$, 89596-92-9; $[(TPP)Co(NO)]^+$, 120544-36-7; (TPP)$FeClO_4$, 57715-43-2; $[(TPP)FeClO_4]^+$, 125138-88-7; $[(TPP)Fe(NO)]^+$, 70622-46-7; (TPP)$CoClO_4$, 76402-67-0; $[(TMP)Fe(NO)]^+$, 117470-06-1; $[(OEP)FeClO_4]^+$, 111436-54-5; (TMP)Fe(NO), 117470-05-0; (TMP)$FeClO_4$, 93862-22-7; $[(TPP)CoClO_4]^+$, 125138-89-8; $[(TMP)FeClO_4]^+$, 125138-90-1; (OEP)Fe, 61085-06-1; (TPP)Co, 14172-90-8; (TPP)Fe(NO), 52674-29-0; CH_2Cl_2, 75-09-2.

(45) Shimomura, E. T.; Phillippi, M. A.; Goff, H. M. *J. Am. Chem. Soc.* **1981**, *103*, 6778.
(46) Truxillo, L. A.; Davis, D. G. *Anal. Chem.* **1975**, *47*, 2260.
(47) Kadish, K. M.; Bottomley, L. A. *Inorg. Chem.* **1980**, *19*, 832.
(48) Swistak, C.; Mu, X. H.; Kadish, K. M. *Inorg. Chem.* **1987**, *26*, 4360.
(49) Kadish, K. M.; Lin, X. Q.; Han, B. C. *Inorg. Chem.* **1987**, *26*, 4161.
(50) Salehi, A.; Oertling, W. A.; Babcock, G. T.; Chang, C. K. *J. Am. Chem. Soc.* **1986**, *108*, 5630.
(51) Fajer, J. Private communication.

Contribution from the Department of Chemistry, University of Houston, Houston, Texas 77204-5641

Synthesis, X-ray Structure, and Characterization of $[(OEP)IrCl]_2$dppe, Where OEP Is the Dianion of Octaethylporphyrin and dppe Is 1,2-Bis(diphenylphosphino)ethane

K. M. Kadish,* Y. J. Deng, and J. D. Korp

Received June 7, 1989

The synthesis and characterization of $[(OEP)IrCl]_2$dppe, where OEP is the dianion of octaethylporphyrin and dppe is 1,2-bis(diphenylphosphino)ethane, are reported. $[(OEP)IrCl]_2$dppe was synthesized from a reaction involving (OEP)$Ir(C_3H_7)$ and dppe in CH_2Cl_2. The bimetallic complex is not generated in benzene solvent, where (OEP)$Ir(C_3H_7)$(dppe) is quantitatively formed instead. Single-crystal X-ray analysis showed $[(OEP)IrCl]_2$dppe to crystallize in the monoclinic space group $P2_1/c$ with cell constants a = 13.989 (4) Å, b = 19.864 (6) Å, c = 17.752 (6) Å, β = 101.22 (2)°, and Z = 2. The Ir atom is out of the porphyrin plane by 0.076 Å toward phosphorus. The compound exhibits a normal UV-visible spectrum in nonaqueous media, as opposed to the hyperspectrum of other Ir(III) porphyrins containing bound phosphine ligands. ^1H NMR data show that all the porphyrin ring protons of $[(OEP)IrCl]_2$dppe are shifted upfield compared to those of monomeric iridium(III) porphyrins, thus suggesting a mutual influence of the ring current. The ethylene group in the bridging dppe ligand is shielded by the two porphyrin moieties, which results in an unusual upfield resonance at −5.74 ppm. $[(OEP)IrCl]_2$dppe undergoes two reversible oxidations and one irreversible reduction in methylene chloride or *n*-butyronitrile at room temperature. The first oxidation involves an overall two-electron-transfer process where one electron is abstracted from each porphyrin ring of the dimer. The product of this reversible oxidation is a biradical, which was characterized by ESR spectroscopy and spectroelectrochemistry. The reduction of $[(OEP)IrCl]_2$dppe in *n*-butyronitrile involes an ECE type mechanism, and the formation of $[(OEP)Ir]^-$ is postulated to occur on the thin-layer spectroelectrochemical time scale after the overall addition of four electrons. However, on the bulk electrolysis time scale, a demetalation of reduced $[(OEP)IrCl]_2$dppe is observed.

Introduction

The electrochemistry of bimetallic porphyrins of the type $[(P)Fe]_2L$ and $[(P)RhCl]_2L$ has been investigated for complexes with both single-atom[1-3] and multiatom[4,5] bridging ligands, L. For some of these porphyrins, there is an interaction across the bridging ligand, while, for others, the two metalloporphyrins are noninteracting. For example, $[(P)Fe]_2L$, where P = the dianion of a given porphyrin and L = C, N, or O, shows significant ligand-mediated metal-metal interactions[1-3] but $[(TPP)Fe]_2L$, when L = pyrazine or 1,2-bis(4-pyridyl)ethylene, shows no interaction between the two iron porphyrin fragments.[5] A recent electrochemical investigation of $[(P)RhCl]_2L$ indicates that the two rhodium porphyrin units can interact when they are connected by a conjugated dibasic nitrogen bridging ligand such as 4,4-bipyridine or *trans*-1,2-bis(4-pyridyl)ethylene.[4] However, when the two Rh(III) complexes are bridged by a nonconjugated dibasic nitrogen bridging ligand such as 1,2-bis(4-pyridyl)ethane or 4,4′-trimethylenebis(pyridine), little if any interaction exists between the two metalloporphyrins.[4] Similar results have been obtained for other non-porphyrin complexes such as $\{[(NH_3)_5Ru]_2L\}^{n+}$ where n = 4, 5, or 6 and L = a 4,4′-dipyridyl type ligand.[6,7]

Bridged bimetallic porphyrins with other central metals or with different types of bridging ligands have not been electrochemically

(1) Lançon, D.; Kadish, K. M. *Inorg. Chem.* **1984**, *23*, 3942.
(2) Kadish, K. M.; Rhodes, R. K.; Bottomley, L. A.; Goff, H. M. *Inorg. Chem.* **1981**, *20*, 3195.
(3) Chang, D.; Cocolios, P.; Wu, Y. T.; Kadish, K. M. *Inorg. Chem.* **1984**, *23*, 1629.
(4) Liu, Y. H.; Anderson, J. E.; Kadish, K. M. *Inorg. Chem.* **1988**, *27*, 2320.
(5) Bottomley, L. A.; Gorce, J.-N. *Inorg. Chem.* **1988**, *27*, 3733.
(6) Creutz, C.; Taube, H. *J. Am. Chem. Soc.* **1969**, *91*, 3988.
(7) (a) Callahan, R. W.; Brown, G. M.; Meyer, T. J. *Inorg. Chem.* **1975**, *14*, 1443. (b) *J. Am. Chem. Soc.* **1974**, *96*, 7829.

0020-1669/90/1329-1036$02.50/0